Multinuclear non-heme iron complexes for double-strand DNA cleavage

Megens, Rik P.; van den Berg, Tieme A.; de Bruijn, Anne; Feringa, B.L.; Roelfes, Gerard

Published in:
Chemistry

DOI:
10.1002/chem.200801409

Publication date:
2009

DOI: 10.1002/chem.200801409

Multinuclear Non-Heme Iron Complexes for Double-Strand DNA Cleavage

Rik P. Megens, Tieme A. van den Berg, A. Dowine de Bruijn, Ben L. Feringa,* and Gerard Roelfes*[a]

Abstract: The cytotoxicity of the antitumor drug BLM is believed to be related to the ability of the corresponding iron complex (Fe-BLM) to engage in oxidative double-strand DNA cleavage. The iron complex of the ligand N4Py (Fe-N4Py; N4Py = *N*,*N*-bis(2-pyridyl)-*N*-bis(2-pyridyl)methylamine) has proven to be a particularly valuable spectroscopic and functional model for Fe-BLM. It is also a very active oxidative DNA-cleaving agent. However, like all other synthetic Fe-BLM mimics, it gives only single-strand DNA cleavage. Since double-strand DNA cleavage requires the delivery of two oxidizing equivalents to the DNA, it was envisaged that multinuclear iron complexes might be capable of effecting double-strand cleavage. For this purpose, a series of ditopic and tritopic N4Py-derived ligands has been synthesized and the corresponding iron complexes have been evaluated for their efficacy in the oxidative cleavage of supercoiled pUC18 plasmid DNA. The dinuclear iron complexes showed significantly enhanced double-strand cleavage activity compared to mononuclear Fe-N4Py, which was relatively independent of the structure of the linking moiety. Covalent attachment of a 9-aminoacridine intercalator to a dinuclear complex did not give rise to improved double-strand DNA cleavage. The most efficient oxidative double-strand cleavage agents proved to be the trinuclear iron complexes. This is presumably the result of increased probability of the simultaneous delivery of two oxidizing equivalents to the DNA.

Keywords: artificial nucleases · DNA cleavage · double-strand cleavage · iron · multitopic complexes

Introduction

Bleomycins (BLMs) are a class of glycopeptide antibiotics that are isolated from *Streptomyces Verticillus*.[1] This class consists of 200 structurally related compounds, of which bleomycins A_2 and B_2, under the name Blenoxane, are used in the clinical treatment of head, neck, and testicular cancers.[2–5] Both in vivo and in vitro, the iron complex of bleomycin (Fe-BLM) is capable of inducing both single-strand and double-strand DNA cleavage.[1,6] The cytotoxicity of BLM is believed to be mainly the result of the double-strand DNA cleavage activity and only to a lesser extent caused by single-strand DNA cleavage.[7]

It is important to recognize that single-strand DNA (ssDNA) cleavage and double-strand DNA (dsDNA) cleavage represent different pathways. Single-strand DNA cleavage is obtained when one oxidation equivalent is delivered to DNA and, through a cascade of reactions, causes a single strand of DNA to break: a nick. When the DNA-cleaving agent does not exhibit sequence selectivity, that is, it cleaves the DNA at random positions, it will continue to nick the DNA until a new nick is sufficiently close to an existing nick in the opposite strand to cause the DNA to separate. Since this is a statistical process, a DNA ds break will only occur after extensive ss cleavage. In vivo, a single-strand DNA break is rapidly repaired by the cellular repair mechanisms.[7]

Double-strand DNA cleavage is the result of two successive strand scissions in opposite strands in close proximity to each other, resulting in a double-strand break.[8] This pathway requires the delivery of two oxidizing equivalents to the DNA helix. BLM is capable of doing this, although the precise nature of the oxidizing species is still under debate.[9] Although repair of double-strand DNA cleavage is possible,[10] repair of single-strand DNA cleavage is much more likely to occur.[7]

[a] R. P. Megens, Dr. T. A. van den Berg, A. D. de Bruijn, Prof. Dr. B. L. Feringa, Dr. G. Roelfes
Stratingh Institute for Chemistry
University of Groningen
Nijenborgh 4, 9747 AG Groningen (The Netherlands)
Fax: (+31) 50-363-4296
E-mail: b.l.feringa@rug.nl
j.g.roelfes@rug.nl

Supporting information for this article is available on the WWW under http://dx.doi.org/10.1002/chem.200801409.

Much effort has been devoted to mimicking the chemistry of Fe-BLM with synthetic model complexes.[11–22] Many of these complexes have proven to be capable of cleaving DNA in the presence of a metal source and O_2.[15,16] However, all of these synthetic mimics have proven to be capable only of effecting single-strand DNA cleavage.[23]

In our group, the pentadentate ligand *N*,*N*-bis(2-pyridylmethyl)-*N*-bis(2-pyridyl)methylamine (N4Py, **1**; Figure 1) has been designed as a mimic of the metal-binding domain of BLM.[24–26] Its acridine-tethered derivative has proven to be an efficient DNA-cleaving agent when using O_2 as terminal oxidant, without requiring addition of a sacrificial reductant.[24] However, as with other synthetic BLM mimics, only single-strand DNA cleavage was achieved.

Since double-strand cleavage requires the delivery of two oxidizing equivalents to the DNA, we hypothesized that covalently linking two single-strand cleaving agents, for example, Fe-N4Py, might effectively give rise to double-strand cleaving agents.[27] Recently, we reported on a binuclear iron complex, based on N4Py, that showed significantly enhanced double-strand cleavage activity.[28]

Multinuclear copper complexes have also been investigated in relation to DNA cleavage.[29–37] It has been reported that dinuclear copper complexes show increased activity compared to their mononuclear counterparts. Moreover, with these dinuclear complexes, selective cleavage at junctions between single- and double-strand DNA was observed. In a related study, a relationship was observed between DNA-cleavage activity and the relative orientation of the copper complexes. Covalent attachment of a third copper complex, that is, formation of a trinuclear copper complex, led to reduced activity.[37]

Here, we present a study on the design of di- and tritopic ligands and their effect on iron-catalyzed oxidative DNA cleavage. Furthermore, efforts have been made to further increase the double-strand cleavage activity by covalent attachment of a 9-aminoacridine DNA binding moiety to a dinuclear complex.

Results and Discussion

Synthesis of the ligands: The ligands employed in this study are shown in Figure 1. In all cases, the ligands were prepared starting from a common precursor, that is, N4Py propyl amine **9**.[24] The ditopic ligands **2**–**4** and the tritopic ligand **7** were prepared in moderate to good yields by reaction of **9** with the appropriate *N*-hydroxysuccinimide-activated esters **10**–**13**, following a procedure reported previously (Scheme 1).[28]

For the synthesis of the tritopic ligand **8** with a flexible core, a slightly modified approach was used (Scheme 2). The core moiety was prepared starting from 4-ketopimelic acid. Benzyl-protection of the carboxylic acid groups was fol-

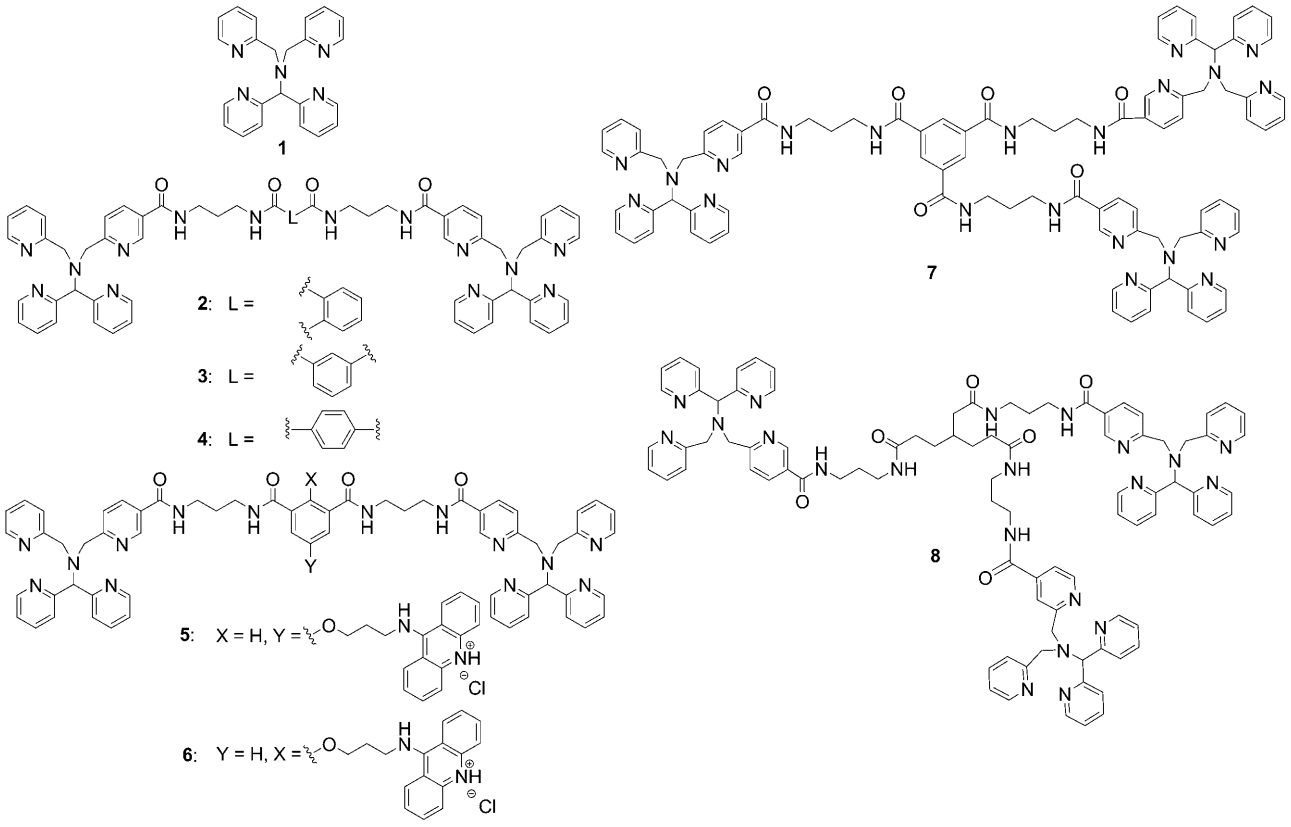

Figure 1. Ligands used in this study.

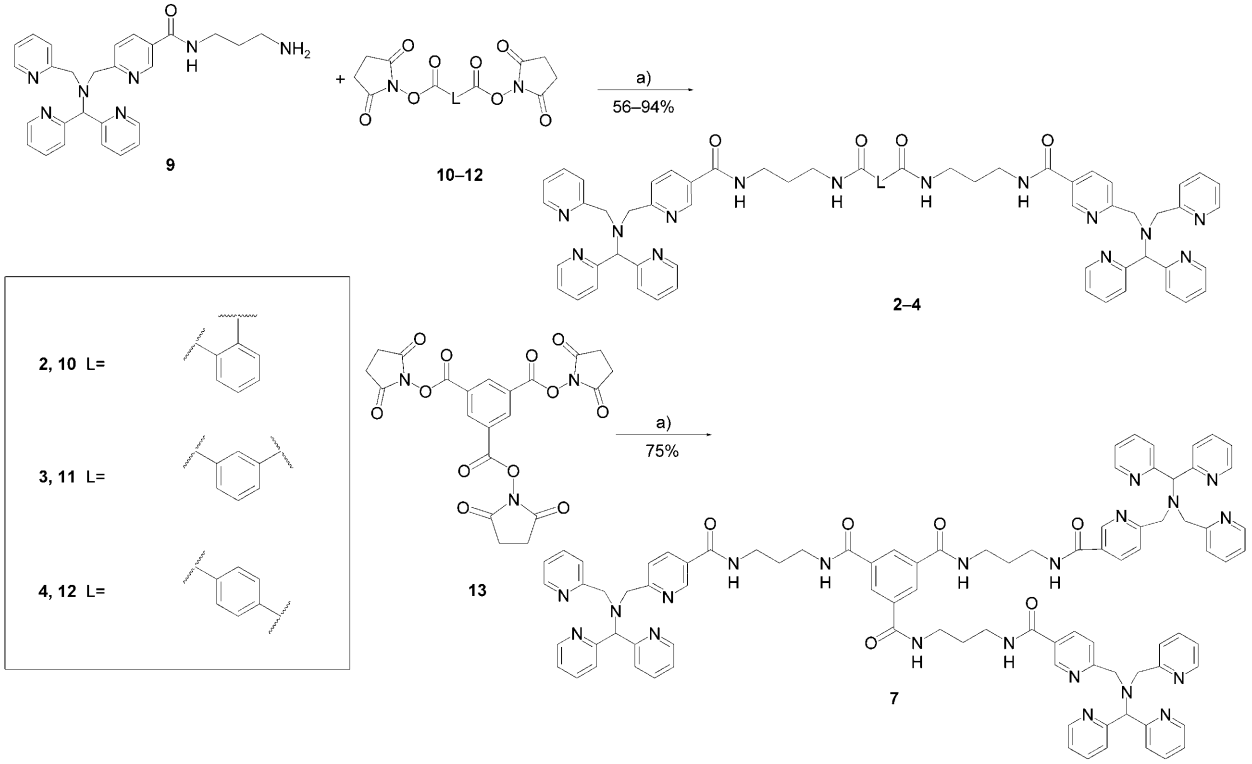

Scheme 1. Synthesis of ditopic N4Py ligands **2–4, 7**. Reagents and conditions: a) CH_2Cl_2, overnight.

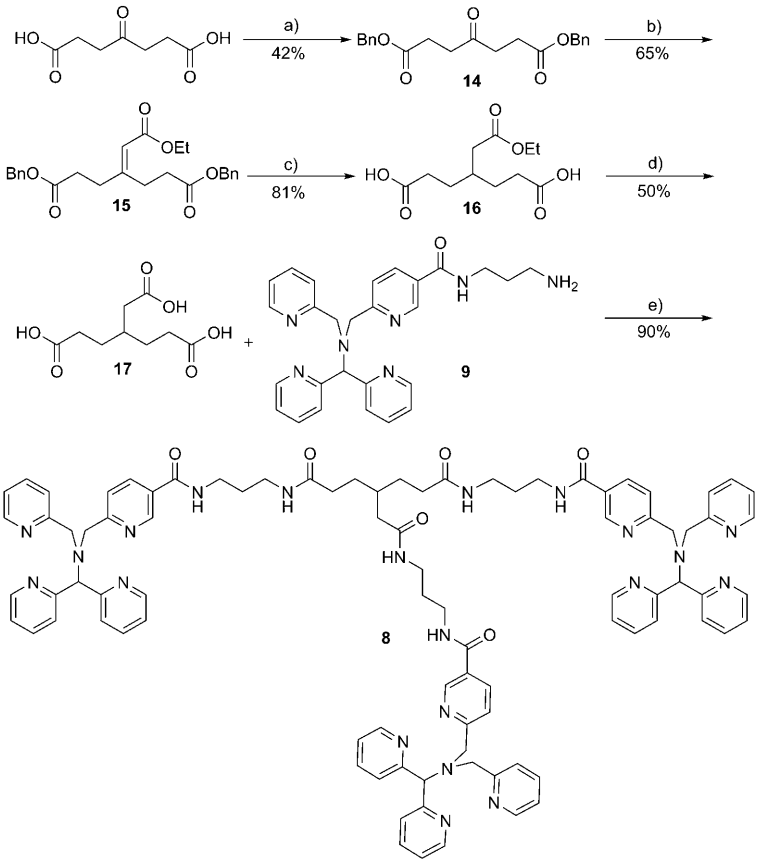

Scheme 2. Synthesis of tritopic ligand **8**. a) Cs_2CO_3, benzyl bromide, DMF, 24 h; b) triethylphosphonoacetate, NaH, THF, 0 °C, then **14**, RT, 1 h, reflux overnight; c) Pd/C, H_2, MeOH, overnight; d) LiOH, MeOH/H_2O, overnight; e) EDC, HOBt, DIEA, CH_2Cl_2, 1 h at 0 °C, then RT overnight.

lowed by a Horner–Wadsworth–Emmons reaction between **14** and triethyl phosphonoacetate to give compound **15**. Hydrogenation of **15** resulted in reduction of the double bond with concomitant removal of the two benzyl protecting groups. Finally, hydrolysis of **16** yielded the triacid **17**. Coupling of triacid **17** with **9** in the presence of EDC, HOBt, and *N*,*N*-diisopropylethylamine (DIEA) in dichloromethane[38] was found to be most efficient; the target tritopic ligand **8** was obtained in an excellent yield of 90%.

The first step towards the acridine-containing target ligands **5** and **6** was the synthesis of the corresponding alkylated isophthalic acid derivatives **18** and **19**. The synthesis of **18** required the use of dimethyl 5-hydroxyisophthalate as starting material, since the free diacid (5-hydroxyisophthalate) was found to be unreactive with regard to alkylation (Scheme 3). The re-

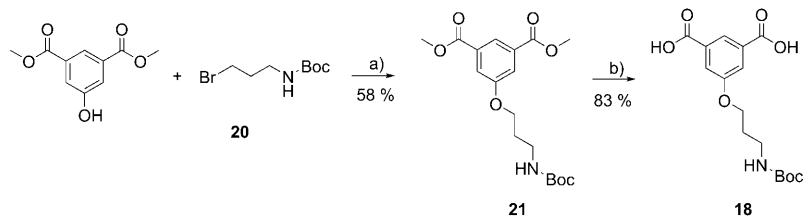

Scheme 3. Synthesis of alkylated isophthalic acid **18**. a) K_2CO_3, acetone, reflux overnight; b) LiOH, THF/H_2O 1:1, 48 h.

action between dimethyl 5-hydroxyisophthalate and Boc-protected aminopropyl bromide **20** in acetone in the presence of K_2CO_3 furnished **21**, hydrolysis of which yielded the diacid **18**.

The synthesis of isomer **19** proved to be somewhat more laborious (Scheme 4). First, 2-methoxyisophthalic acid was converted into the corresponding dimethyl ester **22**. Removal of the methyl of the methoxy group by reaction with BBr_3 in dry CH_2Cl_2 at −80 °C yielded dimethyl 2-hydroxyisophthalate (50 % over two steps; **23**). Finally, alkylation of the alcohol with Boc-protected bromopropylamine **20** in DMF in the presence of K_2CO_3 yielded **24**, which was hydrolyzed to the desired diacid **19**.

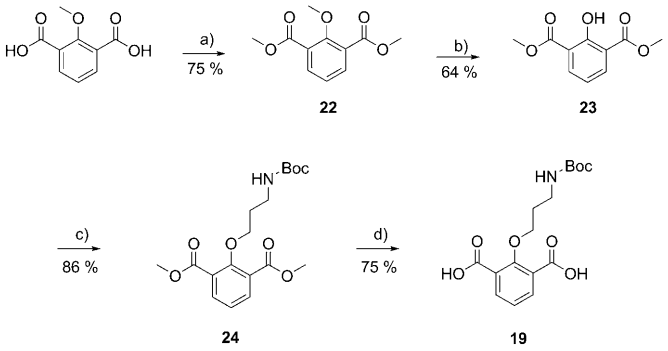

Scheme 4. Synthesis of alkylated isophthalic acid **19**. a) conc. H_2SO_4, MeOH, overnight; b) BBr_3, CH_2Cl_2, −78 °C, 45 min; c) **20**, K_2CO_3, DMF, reflux overnight; d) LiOH, THF/H_2O 1:1, 24 h.

Peptide coupling conditions (EDC/HOBt/*N*,*N*-diisopropylethylamine) for the reactions between the dialkylated isophthalic acids **18** and **19** and N4Py propylamine **9** furnished **25** and **26** in quantitative and 70 % yields, respectively (Scheme 5). The Boc protecting group was removed by overnight treatment with a 10 % solution of TFA in CH_2Cl_2. The isolation of **27** and **28** was complicated by the high solubility of these compounds in water. The final step involved coupling of the free amines with 9-chloroacridine.[24] The resulting ditopic ligands **5** and **6** were isolated as their HCl salts in quantitative yields. After treatment with aqueous NaOH the free base was obtained, which was used for characterization. The HCl salts of **5** and **6** showed good stability; no signs of degradation were observed after prolonged storage. In contrast, the free base showed signs of degradation within a few days.

Complexation: The corresponding iron(II) complexes **29**–**36** of the ligands **1**–**8** were generated in situ by complexation with $(NH_4)_2Fe^{II}(SO_4)_2{\cdot}6H_2O$ immediately prior to use (Scheme 6).

The uptake of one iron(II) ion per N4Py moiety was confirmed by titration of $(NH_4)_2Fe^{II}(SO_4)_2$ against a selection of ligands, with monitoring by ^1H NMR, comparing the relative area of the absorption at $\delta = 25.2$ ppm with that of acetone, as well as by UV/Vis spectrophotometry. A typical example is shown in Figures 2 and 3, indicating binding of three Fe^{II} ions to the ligand **7**.[39]

DNA cleavage with the dinuclear complexes: The DNA cleavage activities of the Fe^{II} complexes **29**–**36** were studied using supercoiled pUC18 plasmid at 37 °C. Although DNA cleavage activity was also observed in the absence of reducing agents, the experiments were carried out in the presence of 1 mM dithiothreitol (DTT) as a reductant to increase the rate of DNA cleavage. The final concentration of the cleaving agent was 1 μM based on Fe^{II}, with a stoichiometry of 1:150 with respect to DNA base pairs. This corresponds to a catalyst loading of 0.6 mol %.

Figure 4 shows the time dependences of the DNA cleavage activities for the iron complexes **29** (mononuclear) and **31** (dinuclear). Extensive DNA cleavage was observed with all of the complexes. The main difference was in the amount of linear DNA that was formed during the reaction. With the dinuclear complexes **30**–**32**, a sudden increase in the amount of linear DNA was observed after about 10 min, which was not seen with Fe^{II}-N4Py (**29**). After 60 min, the fractions of linear DNA were 5 % and 30 % for **29** and **31**, respectively. Beyond this time, the complexes remained active and continued to cleave DNA, but the DNA cleavage activity could no longer be quantified.[6,40] The same reactivity pattern has been observed previously with other N4Py-based dinuclear complexes having different linking moieties.[28] In the case of complexes **30**–**32**, approximately equal amounts of linear DNA were produced,[39] indicating that these complexes show comparable activities towards double-strand DNA cleavage.

The numbers of single-strand and double-strand cuts were determined for each sample by statistical analysis using the Poisson distribution.[41] Figure 5 shows a plot of the number of double-strand breaks (m) versus the number of single-strand breaks (n) for the complexes **29**–**32**. From this plot, it is quite clear that complex **29** is a typical single-strand cleaving agent since it follows the Freifelder–Trumbo relationship, which describes a purely single-strand cleaving pathway.[8] In other words, double-strand cleavage occurs only after extensive nicking of supercoiled DNA has taken place. The plots for complexes **30**–**32** initially follow the Freifelder–Trumbo relationship, but then suddenly show a strong in-

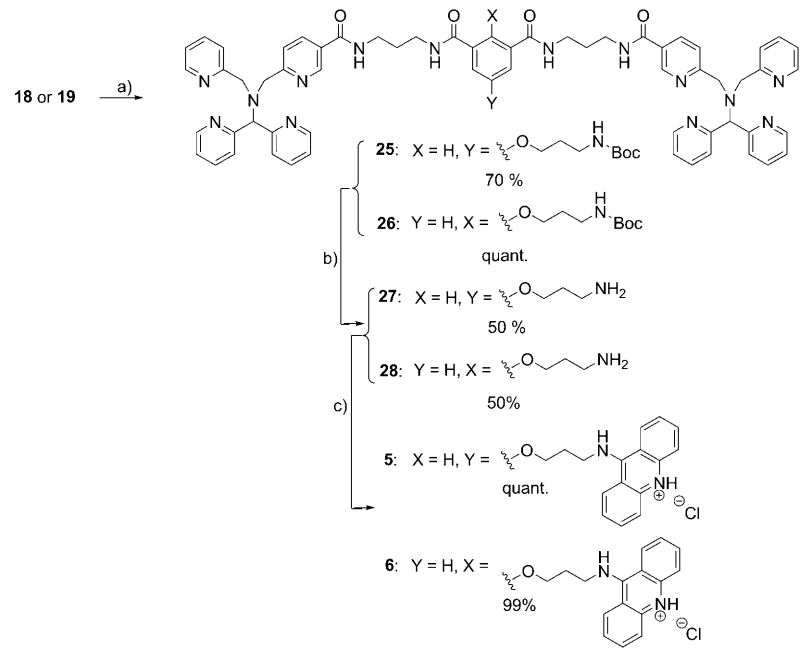

Scheme 5. Synthesis of ligands **5** and **6**. a) **9**, HOBt, DIEA, EDC, CH_2Cl_2, overnight; b) 10% TFA in CH_2Cl_2, overnight; c) 9-chloroacridine, phenol, 80°C, 3 h.

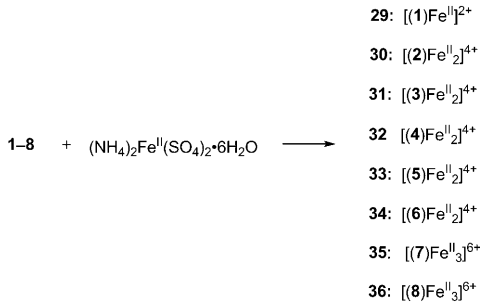

Scheme 6. Complexation with Fe^{II} salts.

crease in the number of double-strand cuts (m) with respect to the number of single-strand cuts (n). This is a clear indication that more linear DNA is formed via a direct double-strand DNA cleavage pathway. Such a sudden increase in ds cleavage activity has been observed previously, whereupon it was demonstrated that the dinuclear iron complexes were more efficient in bringing about double-strand cleavage of nicked DNA than that of supercoiled DNA.[28] In view of their structural similarity to the present complexes, this is most likely the case here as well.

Nearly identical m/n ratios were calculated for **30**–**32**, within the uncertainty limits of the data. Apparently, the topology of the dinuclear complexes has little influence on the DNA oxidation activity or on the type of cleavage pathway. In this respect, the dinuclear iron complexes behave differently to the previously studied dinuclear copper complexes. Guo and co-workers found clear differences in the DNA oxidation activities between 1,3- and 1,4-disubstituted phenyl-based dicopper complexes.[37] The differences between these complexes were rationalized by assuming a cooperative interaction between the two copper centers to activate dioxygen (or hydrogen peroxide) in the case of the 1,3-substitution pattern. The fact that the DNA-cleavage results with the present dinuclear iron complexes are not dependent on ligand topology suggests that the two iron centers activate dioxygen independently.

In an attempt to further increase the activity and double-strand cleavage selectivity, ditopic Fe-N4Py complexes **33** and **34** containing a DNA-intercalating 9-aminoacridine moiety were prepared and tested. In the case of mononuclear iron complexes, this gave rise to significantly enhanced DNA-cleavage activity.[24]

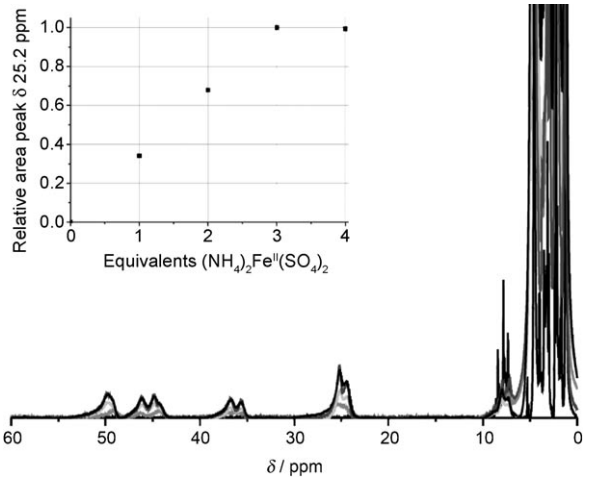

Figure 2. ^1H NMR titration of **7** in D_2O with $(NH_4)_2Fe^{II}(SO_4)_2$ (——) 0 equiv Fe^{II}, (——) 1 equiv Fe^{II}, (——) 2 equiv Fe^{II}, (——) 3 equiv Fe^{II}, and (——) 4 equiv Fe^{II}. Inset: Plot of the relative area of the absorption at $\delta = 25.2$ ppm compared to the acetone peak against the number of equivalents of $(NH_4)_2Fe(SO_4)_2$.

Depending on the substitution pattern of the central phenyl core, significantly different results were obtained in the DNA-cleavage experiments. A much slower consumption of supercoiled DNA was observed for **33** ($t_{1/2} \approx 25$ min) compared to **34** ($t_{1/2} \approx 10$ min). The rate of consumption of supercoiled DNA by the latter complex was comparable to that by dinuclear complexes not bearing the acridine moiety (see above). Furthermore, hardly any linear DNA was produced within 1 h when **33** was employed as catalyst (Fig-

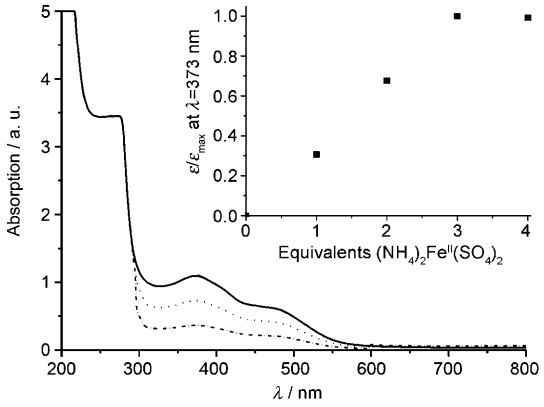

Figure 3. UV/Vis spectra of ligand **7** (0.06 mM) after addition of (–•–•) 1 equiv, (•••••) 2 equiv, (-----) 3 equiv, and (——) 4 equiv of $(NH_4)_2Fe^{II}(SO_4)_2$. Inset: Plot of the $\varepsilon/\varepsilon_{max}$ ratio at 356 nm against the number of equivalents of $(NH_4)_2Fe^{II}(SO_4)_2$.

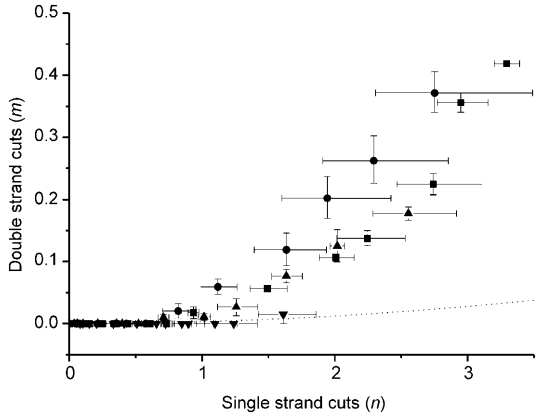

Figure 5. Number of double-strand cuts per DNA molecule (m) as a function of the number of single-strand cuts per DNA molecule (n) for **29** (▼), **30** (■), **31** (●), and **32** (▲). The dotted line is the Freifelder–Trumbo relationship.[8] Error bars represent the uncertainty of the data, based on a Monte Carlo simulation, taking into account a standard deviation σ of 0.03.[39]

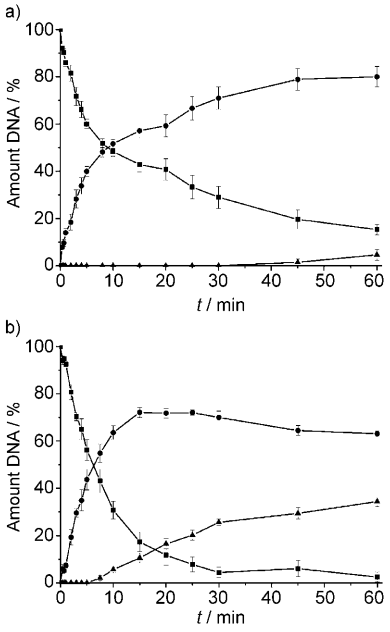

Figure 4. Temporal evolution of the aerobic oxidation of supercoiled plasmid DNA (■) to nicked DNA (●) and linear DNA (▲) under catalysis by a) $[(\mathbf{1})Fe^{II}]^{2+}$ (**29**) and b) $[(\mathbf{3})Fe^{II}_2]^{4+}$ (**31**). Error bars represent the root-mean-square (rms) error based on three runs. A correction factor of 1.31 was used to compensate for the reduced ethidium bromide uptake capacity of supercoiled DNA.[28]

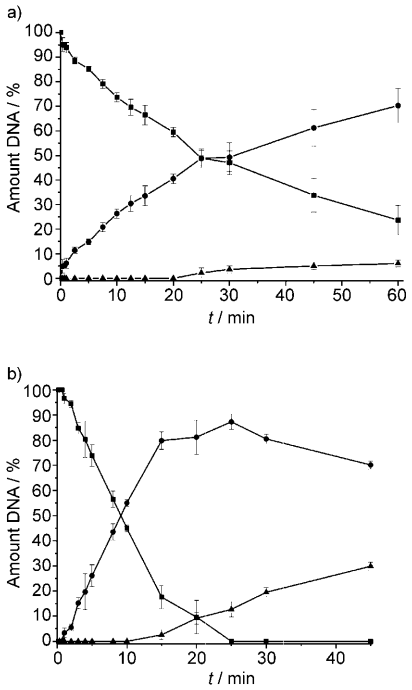

Figure 6. Temporal evolution of the aerobic oxidation of supercoiled plasmid DNA (■) to nicked DNA (●) and linear DNA (▲) under catalysis by a) $[(\mathbf{5})Fe^{II}_2]^{4+}$ (**33**) and b) $[(\mathbf{6})Fe^{II}_2]^{4+}$ (**34**). Error bars represent the root-mean-square (rms) error based on three runs. A correction factor of 1.31 was used to compensate for the reduced ethidium bromide uptake capacity of supercoiled DNA.

ure 6a), whereas more than 30% of linear DNA was formed within the same period with **34** (Figure 6b).

A plot of the average number of double-strand versus single-strand DNA cuts for **33** and **34** (Figure 7) shows a similar pattern for both complexes; initially, the Freifelder–Trumbo relationship (dashed line) is followed, implying a single-strand cleavage pathway. In the later stages of the reaction, double-strand cleavage activity is observed, similar to what was seen with **30**–**32**, albeit with less efficiency.

Interestingly, complex **34** displayed double-strand DNA cleavage even in the early phase of the reaction ($n>0.5$), whereas complex **33** required a higher number of single-strand cuts ($n\approx2$) before double-strand DNA cleavage commenced.

The observed difference between the acridine complexes is most likely related to the relative positioning of the acridine moiety with respect to the two Fe(N4Py) moieties. When the acridine of complex **33** (with a 1,3,5-substitution

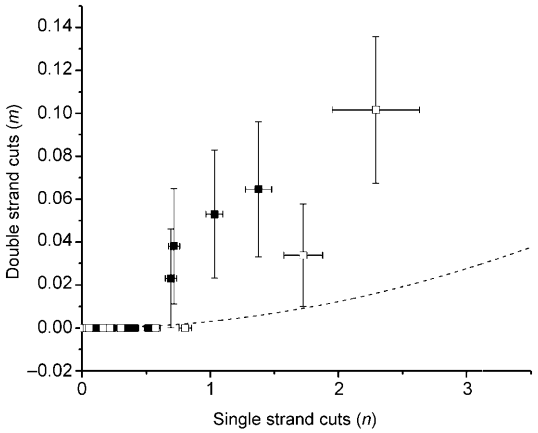

Figure 7. Number of double-strand cuts per DNA molecule (m) as a function of the number of single-strand cuts per DNA molecule (n) for **33** (□) and **34** (■). The dotted line is the Freifelder–Trumbo relationship.[8] Error bars represent the uncertainty of the data, based on a Monte Carlo simulation, taking into account a standard deviation σ of 0.03.

pattern at the central phenyl moiety) intercalates with the DNA, the two active iron moieties are pointing away from the DNA, thus reducing the DNA-cleavage activity. In contrast, due to the 1,2,3-substitution pattern, the iron centers of complex **34** are pointing towards the DNA and can engage in its oxidation. From these results, it is clear that no beneficial effect is obtained from attaching a DNA intercalator; at best the ds cleavage activity is slightly less than that of the binuclear complexes without an acridine moiety. Presumably, the highly cationic binuclear iron complex already has a very strong affinity for DNA and, hence, an additional DNA-binding moiety has no added advantage. However, more research is required to further substantiate these findings.

DNA cleavage with the trinuclear complexes: A similar cleavage pattern was observed for $[(\mathbf{7})Fe^{II}_3]^{6+}$ (**35**) and $[(\mathbf{8})Fe^{II}_3]^{6+}$ (**36**) (Figure 8). Initially, only nicked DNA was formed, and linear DNA was only formed after a short lag period, as was also observed with the dinuclear complexes. It seems that **35**, which has a phenyl core, is more effective in producing linear DNA than the trimer **36** possessing a more flexible core. In the case of **35**, 30% of the DNA is in the linear form after just 30 min. Within the same time, only 20% linear DNA is obtained with **36**; a reaction time of 60 min is required for the fraction of linear DNA to reach 30% (Figure 8). Taken together, these results suggest that both complexes display double-strand cleavage, but that the more rigid complex **35** has higher activity.

As before, a plot of double-strand cuts versus single-strand cuts shows that, initially, only single-strand cuts are observed for both complexes (Figure 9). In the course of the reaction, double-strand cuts are observed as well. Although the trinuclear complex **35** produces double-strand cuts somewhat more quickly than trinuclear complex **36**, this is not reflected in the m/n ratio. This points to a similar cleavage pathway, albeit with different reaction rates. Compari-

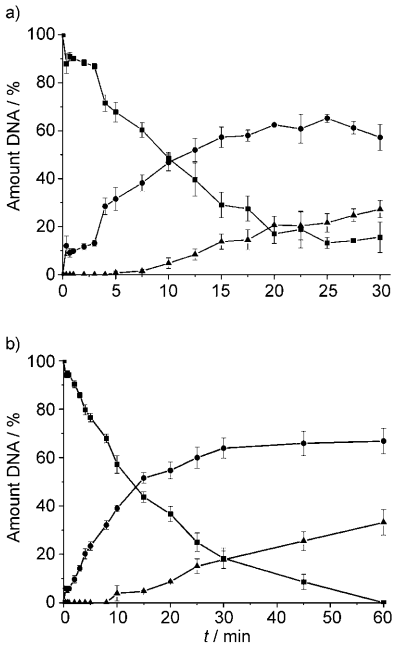

Figure 8. Temporal evolution of the aerobic oxidation of supercoiled plasmid DNA (■) to nicked DNA (●) and linear DNA (▲) under catalysis by a) $[(\mathbf{7})Fe^{II}_3]^{6+}$ (**35**) and b) $[(\mathbf{8})Fe^{II}_3]^{6+}$ (**36**). Error bars represent the root-mean-square (rms) error based on three runs. A correction factor of 1.31 was used to compensate for the reduced ethidium bromide uptake capacity of supercoiled DNA.

son of the results with those obtained for a dinuclear complex, namely the 1,3-substituted phenyl dinuclear complex **31**, revealed a similar trend (Figure 9).

However, for the trinuclear complexes, the introduction of double-strand breaks in the DNA was observed at an earlier stage of the reaction and generally higher m/n ratios were found. This suggests that the trinuclear complexes are

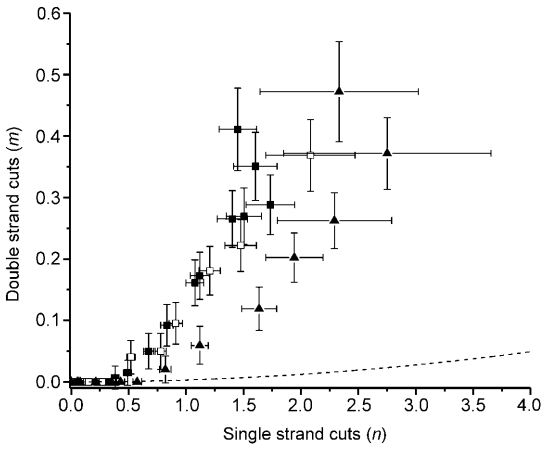

Figure 9. Number of double-strand cuts per DNA molecule (m) as a function of the number single-strand cuts per DNA molecule (n) for **35** (■) and **36** (□). Data for a dinuclear complex are also included (▲, **31**). The dotted line is the Freifelder–Trumbo relationship.[8] Error bars represent the uncertainty of the data, based on a Monte Carlo simulation, taking into account a standard deviation σ of 0.03.

more efficient double-strand cleaving agents, but it should be emphasized that the increase in double-strand cleavage activity is not as large as was observed on going from mononuclear complexes to dinuclear complexes. The higher double-strand cleavage activity is most likely the result of the increased probability of simultaneous delivery of multiple oxidizing equivalents to both DNA strands within 16 base pairs of each other.

Conclusion

In the present study we have shown that oxidative double-strand DNA cleavage activity can be achieved by using multinuclear iron complexes based on the N4Py ligand scaffold. Although these complexes are still not as efficient as Fe-BLM, they are nevertheless are the most efficient synthetic iron-based double-strand DNA-cleaving agents known to date. Compared to mononuclear iron complexes, binuclear iron complexes show significantly enhanced double-strand cleavage activity, which appears to be affected only to a minor extent by the structure of the linking moiety. Covalent attachment of a DNA-binding moiety did not give rise to improved DNA-cleaving agents. However, trinuclear iron complexes did exhibit significantly enhanced ds cleavage activity, with complex **35**, containing a rigid core, being the most efficient. Taken together, the present results demonstrate that by appropriate design of multinuclear non-heme iron complexes, efficient oxidative double-strand DNA cleavage can be achieved.

Experimental Section

Chemicals and methods: All reactions were performed under an inert atmosphere (N_2 or Ar). The N4Py-propylamine **9** was synthesized according to literature procedures and all data were in agreement with those published.[24,42] Syntheses of **10**–**24** can be found in the Supporting Information.

pUC18 plasmid DNA, isolated from *E. coli* XL1 Blue, was purified using QIAGEN maxi kits. Concentrations were determined by means of both dilution gels and UV/Vis (A_{260}). Restriction enzymes and restriction buffers were purchased from New England Biolabs (NEB). Agarose used for the agarose slab gels was purchased from Invitrogen. A solution of number IV dye, consisting of 0.08% bromophenol blue and 40% sucrose (6× conc.) was added to the samples prior to electrophoresis. All gel experiments were run on 1.2% agarose slab gels for at least 90 min at 70 V. Gels were stained in an ethidium bromide bath (1.0 μg mL^{-1}) for 45 min. Pictures of the gel slabs were taken with a Spot Insight CCD camera and handled with the software program Spot (version 3.4). The bands on the film were quantified using the software program Gel-Pro Analyzer version 4.0.00.001.

DNA oxidation reactions: $(NH_4)_2Fe^{II}(SO_4)_2$ (1 equiv per N4Py moiety) was added to solutions of ligands **1**–**8** in H_2O. The respective mixtures and a solution of dithiothreitol (DTT) were simultaneously added to a buffered solution (Tris-HCl, 10 mM, pH 8.0) of supercoiled pUC18 plasmid DNA (0.1 μg μL^{-1}; 150 μM in base pairs) to give a final concentration of 1.0 μM iron complex, based on iron, and 1.0 mM DTT. The mixture, with a final volume of 50 μL, was incubated at 37 °C. At the times indicated, a sample (2 μL) was taken from the reaction mixture, diluted in water (15 μL; containing 1000 equiv of NaCN) and loading buffer (3 μL) and immediately frozen in liquid nitrogen. The samples were analyzed by gel electrophoresis. Results are the average of three independent runs. Statistical analysis was employed to calculate the amounts of ssc and dsc as described previously (see below).[28]

Calculation of the uncertainty in the values by a Monte Carlo method: The uncertainties in the values of n and m were calculated by a Monte Carlo simulation using the software program Mathematica version 5.2.0.0. An algorithm was used to calculate the values of both n and m from 5000 pseudo-random generated fraction sizes of supercoiled, nicked, and linear DNA using the following equations:[6,8]

$$f_m = m \times e^{-m} \quad (1)$$

$$f_I = e^{-(m+n)} \quad (2)$$

$$m = \frac{n^2(2h=1)}{4L} \quad (3)$$

Equation (3) is the Freifelder–Trumbo relationship. In these equations, f_I is the fraction of supercoiled DNA, f_{III} is the fraction of linear DNA, m is the average number of double-strand cuts, n is the average number of single-strand cuts, h is the maximum distance in base pairs between nicks on opposite strands to generate a double-strand cut (i.e. 16), and L is the total number of base pairs of the DNA used (2686 bp for pUC18 plasmid DNA).

These pseudo-random generated fraction sizes are based on the experimentally obtained average value (based on three independent runs) and generated within a normal distribution based on a standard deviation of 0.03. This standard deviation was determined independently by 24 identical DNA oxidation experiments with supercoiled pUC18 plasmid DNA and Fe(N4Py) (vide supra; reaction quenched at $t=30$ min) and is the largest standard deviation in the experiment.

Synthesis of ligands 2–4 and 7 general procedure: Two equivalents of the propylamine-substituted N4Py **9** were added to a solution (0.1 mM in CH_2Cl_2) of one equivalent of the corresponding *N*-hydroxysuccinimide-activated diacid **10**, **11**, or **12**. The mixture was stirred overnight at room temperature. It was then washed with water (3×10 mL) and dried over Na_2SO_4. After filtration, the filtrate was concentrated and the product was precipitated by adding Et_2O. Further purification was achieved by size-exclusion chromatography on a Sephadex LH20 column using MeOH as the mobile phase. The fractions were analyzed by HPLC using method A (see the Supporting Information). After evaporation of the MeOH, the oily product was taken up in the minimum volume of CH_2Cl_2 and the product was precipitated by adding Et_2O.

***N*^{1},*N*^{2}-Bis(3-{[(6-{[[di(2-pyridinyl)methyl](2-pyridinylmethyl)amino]methyl}-3-pyridinyl)carbonyl]amino}propyl)phthalamide (2)**: Starting from **10** (39.3 mg, 0.109 mmol) and **9** (0.102 g, 0.218 mmol), **2** was obtained as a pale light-brown solid (0.101 g, 95 μmol, 94%). ^{1}H NMR (400 MHz, CD_3OD): $\delta=8.78$ (d, $J=2.2$ Hz, 2H), 8.45 (m, 4H), 8.35 (m, 2H), 8.04 (dd, $J=8.1$, 2.2 Hz, 2H), 7.79–7.64 (m, 14H), 7.55 (m, 2H), 7.49 (m, 2H), 7.25 (m, 4H), 7.18 (m, 2H), 5.33 (s, 2H), 3.99 (s, 4H), 3.95 (s, 4H), 3.44 (m, 8H), 1.85 ppm (m, 4H); ^{13}C NMR (50.3 MHz, CD_3OD): $\delta=171.8$, 167.7, 163.8, 160.7, 160.3, 150.0, 149.5, 148.7, 138.5, 138.4, 137.2, 136.9, 131.3, 129.9, 128.8, 125.6, 124.8, 124.1, 124.0, 123.7, 74.2, 58.7, 58.3, 38.3, 38.2, 29.8 ppm; MS (ESI$^+$): m/z: 1065.5 $[M+H]^+$, 895.6 $[M-PyCH_2Py+H]^+$, 533.5 $[M+2H]^{2+}$, 356.1 $[M+3H]^{3+}$.

***N*^{1},*N*^{3}-Bis(3-{[(6-{[[di(2-pyridinyl)methyl](2-pyridinylmethyl)amino]methyl}-3-pyridinyl)carbonyl]amino}propyl)isophthalamide (3)**: Starting from **11** (38 mg, 0.11 mmol) and **9** (0.10 g, 0.21 mmol), **3** was obtained as a pale light-brown oil (65 mg, 0.06 mmol, 56%). ^{1}H NMR (400 MHz, CD_3OD): $\delta=8.83$ (d, $J=1.5$ Hz, 2H), 8.47 (d, $J=4.7$ Hz, 4H), 8.37 (d, $J=4.8$ Hz, 2H), 8.33 (m, 1H), 8.10 (dd, $J=8.1$, 2.2 Hz, 2H), 7.98 (dd, $J=7.7$, 1.8 Hz, 2H), 7.81–7.66 (m, 15H), 7.54 (m, 2H), 7.27 (m, 4H), 7.21 (t, $J=5.9$ Hz, 2H), 5.36 (s, 2H), 4.01 (s, 4H), 3.98 (s, 4H), 3.49 (m, 8H), 1.93 ppm (m, 4H); ^{13}C NMR (50.3 MHz, CD_3OD): $\delta=169.42$, 167.89, 163.86, 160.78, 149.95, 149.50, 148.58, 138.42, 138.35, 136.87, 136.14, 131.16, 129.93, 127.30, 125.62, 124.81, 124.16, 124.00, 123.64, 74.40, 58.77, 58.37, 54.80,

38.43, 30.22 ppm; MS (ESI$^+$): m/z: 1065.5 $[M+H]^+$, 895.6 $[M-PyCH_2Py+H]^+$, 533.5 $[M+2H]^{2+}$, 356.1 $[M+3H]^{3+}$.

N^1,N^4-Bis(3-{[(6-{[[di(2-pyridinyl)methyl](2-pyridinylmethyl)amino]methyl}-3-pyridinyl)carbonyl]amino}propyl)terephthalamide (4): Starting from **12** (38 mg, 0.11 mmol) and **9** (0.10 g, 0.21 mmol), **4** was obtained as a pale light-brown oil (80 mg, 75.4 μmol, 71%). ^{1}H NMR (400 MHz, CD_3OD): $\delta=8.83$ (d, $J=1.5$ Hz, 2H), 8.47 (d, $J=4.8$ Hz, 4H), 8.36 (d, $J=4.8$ Hz, 2H), 8.19 (dd, $J=8.1$, 1.8 Hz, 2H), 7.91 (s, 4H), 7.81–7.66 (m, 14H), 7.35 (m, 4H), 7.28 (t, $J=5.5$ Hz, 2H), 5.36 (s, 2H), 4.03 (s, 4H), 3.98 (s, 4H), 3.48 (dd, $J=6.6$, 6.2 Hz, 8H), 1.92 ppm (t, $J=6.6$ Hz, 4H); ^{13}C NMR (50.3 MHz, CD_3OD): $\delta=169.3$, 167.9, 163.9, 160.8, 160.3, 145.0, 149.5, 148.6, 138.4, 136.9, 129.9, 128.5, 125.6, 124.8, 124.2, 124.01, 123.7, 74.4, 58.8, 58.4, 38.4, 30.2 ppm; MS (ESI$^+$): m/z: 1065.5 $[M+H]^+$, 895.5 $[M-PyCH_2Py+H]^+$, 533.5 $[M+2H]^{2+}$.

5-(*N*-*tert*-Butyloxycarbonyl-3-aminopropoxy)-N^1,N^3-bis(3-{[(6-{[[di(2-pyridinyl)methyl](2-pyridinylmethyl)amino]methyl}-3-pyridinyl)carbonyl]amino}propyl)isophthalamide (25): EDC (0.187 g, 2.04 mmol) and *N*,*N*-diisopropylethylamine (89.9 mg, 115 μL, 0.696 mmol) were added to a mixture of propylamine-N4Py derivative **9** (0.324 g, 0.693 mmol), HOBt (94 mg, 0.696 mmol), and diacid **18** (0.107 g, 0.315 mmol) in CH_2Cl_2 (40 mL). The reaction mixture was stirred overnight at room temperature. Saturated aqueous $NaHCO_3$ solution (20 mL) was then added and the layers were separated. The organic phase was washed with saturated aqueous $NaHCO_3$ solution (2×20 mL) and water (20 mL). Drying over Na_2SO_4, filtration, and evaporation of the solvent yielded a yellow foam (0.417 g, 0.337 mmol, quant.). Optional purification was achieved by size-exclusion chromatography (Sephadex LH 20/MeOH) or preparative RP-HPLC. ^{1}H NMR (400 MHz, CD_3OD): $\delta=8.81$ (dd, $J=2.3$, 0.7 Hz, 2H), 8.46 (m, 4H), 8.35 (ddd, $J=4.9$, 1.7, 0.9 Hz, 2H), 8.09 (dd, $J=8.2$, 2.3 Hz, 2H), 7.88 (m, 1H), 7.82–7.61 (m, 14H), 7.52 (d, $J=1.3$ Hz, 2H), 7.26 (ddd, $J=6.3$, 4.9, 2.4 Hz, 4H), 7.19 (ddd, $J=7.2$, 4.9, 1.4 Hz, 2H), 5.34 (s, 2H), 4.09 (t, $J=6.0$ Hz, 2H), 4.01 (s, 4H), 3.96 (s, 4H), 3.47 (m, 10H), 3.23 (t, $J=6.8$ Hz, 2H), 1.92 (m, 6H), 1.40 ppm (s, 9H); ^{13}C NMR (100 MHz, CD_3OD): $\delta=168.1$, 166.7, 162.7, 159.6, 159.5, 159.1, 157.3, 148.8, 148.3, 147.4, 137.3, 137.2, 136.2, 135.7, 128.8, 124.5, 123.6, 123.0, 122.8, 122.5, 118.1, 116.2, 78.8, 73.2, 65.9, 57.6, 57.2, 37.3, 37.2, 29.4, 29.0, 27.6 ppm; MS (ESI$^+$): m/z: 1260.5 $[M+Na]^+$, 1238.6 $[M+H]^+$, 1068.5 $[M-PyCH_2Py+H]^+$, 620.0 $[M+2H]^{2+}$, 536.0 $[M-PyCH_2Py+2H]^{2+}$, 413.9 $[M+3H]^{3+}$, 395.2 $[M-Boc+2Na+H]^+$, 380 $[M-Boc+3H]^+$.

5-(3-Aminopropoxy)-N^1,N^3-bis(3-{[(6-{[[di(2-pyridinyl)methyl](2-pyridinylmethyl)amino]methyl}-3-pyridinyl)carbonyl]amino}propyl)isophthalamide (27): The Boc-protected di-N4Py ligand **25** (0.417 g, 0.337 mmol) was taken up in CH_2Cl_2 (9 mL), and then TFA (1 mL) was carefully added. After stirring the mixture overnight at room temperature, 2 M aqueous NaOH solution was added until pH > 10. The resulting solution was stirred for an additional 10 min and then extracted with CH_2Cl_2 (3× 20 mL). The combined organic layers were washed with water (3× 20 mL) and dried over Na_2SO_4. Filtration and evaporation of the solvent yielded a yellow-brown oil, which was purified on a Sephadex LH-20 column using MeOH as the mobile phase. A light-brown solid was obtained (0.166 g, 0.146 mmol, 43%). ^{1}H NMR (400 MHz, CD_3OD): $\delta=$ 8.81 (d, $J=2.3$ Hz, 2H), 8.45 (m, 4H), 8.35 (ddd, $J=4.9$, 1.6, 0.89 Hz, 2H), 8.09 (dd, $J=8.2$, 2.3 Hz, 2H), 7.89 (t, $J=1.5$ Hz, 1H), 7.82–7.62 (m, 14H), 7.53 (d, $J=1.5$ Hz, 2H), 7.26 (ddd, $J=6.3$, 4.9, 2.4 Hz, 4H), 7.19 (ddd, $J=7.2$, 4.9, 1.4 Hz, 1H), 5.34 (s, 2H), 4.15 (t, $J=6.1$ Hz, 2H), 4.01 (s, 4H), 3.96 (s, 4H), 3.47 (m, 8H), 2.89 (t, $J=7.0$ Hz, 2H), 1.99 (m, 2H), 1.90 ppm (dd, $J=6.4$, 6.3 Hz, 4H); ^{13}C NMR (75.5 MHz, CD_3OD): $\delta=$ 168.0, 166.7, 162.7, 159.6, 159.4, 159.1, 148.8, 148.4, 147.4, 137.24, 137.18, 136.3, 135.7, 128.8, 124.5, 123.7, 123.0, 122.8, 122.6, 122.5, 118.2, 116.2, 73.3, 66.3, 57.6, 57.2, 38.2, 37.3, 37.2, 31.1, 29.0 ppm; MS (ESI$^+$): m/z: 1160.5 $[M+Na]^+$, 1138.8 $[M+H]^+$, 968.6 $[M-PyCH_2Py+H]^+$, 570.5 $[M+2H]^{2+}$, 380.5 $[M+3H^+]^{3+}$.

5-[3-(9-Acridinylamino)propoxy]-N^1,N^3-bis(3-{[(6-{[[di(2-pyridinyl)methyl](2-pyridinylmethyl)amino]methyl}-3-pyridinyl)carbonyl]amino}propyl)isophthalamide (5): A mixture of **27** (92 mg, 81 μmol), 9-chloroacridine (17.3 mg, 81 μmol), and phenol (1.0 g) was heated at 80 °C for 3 h. After cooling to room temperature, Et_2O (10 mL) was added, which resulted in the formation of a yellow-brown precipitate. After stirring for 5 min, the Et_2O was decanted off and fresh Et_2O (10 mL) was added. The yellow suspension was stirred overnight. After decanting off the Et_2O once more, further fresh Et_2O (10 mL) was added and the suspension was placed in an ultrasonic bath for 10 min. After stirring for an additional 1 h, the Et_2O was removed and the yellow solid was isolated and dried. This HCl salt of the product was recovered in quantitative yield. A portion of this yellow solid (100 mg) was taken up in 2 M aqueous NaOH (10 mL) and the solution was extracted with CH_2Cl_2 (3×10 mL). The combined organic phases were washed with 2 M NaOH (3×10 mL) and dried over Na_2SO_4. Filtration and evaporation of the solvent yielded a yellow oil (95 mg, quantitative). An optional purification step by preparative RP-HPLC yielded pure material. ^{1}H NMR (400 MHz, CD_3OD): $\delta=$ 8.80 (dd, $J=2.3$ Hz, 0.5 Hz, 2H), 8.44 (m, 4H), 8.33 (ddd, $J=5.0$, 1.4, 0.9 Hz, 2H), 8.29 (d, $J=8.7$ Hz, 2H), 8.07 (dd, $J=8.2$, 2.3 Hz, 2H), 7.83 (t, $J=1.4$ Hz, 1H), 7.81–7.55 (m, 20H), 7.35 (d, $J=1.4$ Hz, 2H), 7.30 (ddd, $J=8.7$, 6.9, 1.4 Hz, 2H), 7.24 (ddd, $J=6.0$, 4.9, 2.6 Hz, 4H), 7.16 (ddd, $J=6.9$, 5.0, 1.5 Hz, 2H), 5.33 (s, 2H), 4.15 (t, $J=5.6$ Hz, 2H), 4.11 (t, $J=6.6$ Hz, 2H), 3.99 (s, 4H), 3.94 (s, 4H), 3.46 (m, 8H), 2.28 (m, 2H), 1.89 ppm (m, 4H); ^{13}C NMR (100 MHz, CD_3OD): $\delta=167.9$, 166.7, 162.7, 159.6, 159.1, 159.0, 153.7, 148.8, 148.3, 147.4, 137.22, 137.16, 136.2, 135.7, 130.7, 128.7, 126.5–126.0, 124.4, 123.9, 123.6, 123.0, 122.8, 122.5, 122.4, 118.2, 116.02, 115.97, 73.2, 65.9, 57.6, 57.2, 48.7, 37.24, 37.18, 30.3, 29.0 ppm (signals missing due to peak overlap); MS (ESI$^+$): m/z: 1337.5 $[M+Na]^+$, 1315.6 $[M+H]^+$, 680.6 $[M+2Na]^{2+}$, 669.6 $[M+Na+H]^{2+}$, 658.6 $[M+2H]^{2+}$, 570.1 $[M-acridine+2H]^{2+}$, 454.0 $[M+2Na+H]^{3+}$, 446.8 $[M+Na+2H]^{3+}$, 439.5 $[M+3H]^{3+}$; HRMS (ESI$^+$): calcd for $C_{78}H_{76}N_{16}O_5$ $[M+2H]^{2+}$: m/z 658.309; found: 658.308, calcd for $C_{78}H_{77}N_{16}O_5$ $[M+3H]^{3+}$: m/z 439.209; found 439.210.

2-(*N*-*tert*-Butyloxycarbonyl-3-aminopropoxy)-N^1,N^3-bisisophthalamide (26): EDC (0.180 g, 1.16 mmol) and *N*,*N*-diisopropylethylamine (0.14 mL, 0.825 mmol) were added to a mixture of propylamine-N4Py derivative **9** (350 mg, 0.75 mmol), HOBt (112 mg, 0.825 mmol), and diacid **19** (127 mg, 0.375 mmol) in CH_2Cl_2 (10 mL). The reaction mixture was stirred overnight at room temperature. The solvent was then removed and fresh CH_2Cl_2 (20 mL) was added. The solution was washed with saturated aqueous $NaHCO_3$ solution (3×20 mL) and water (3×20 mL), and then dried over Na_2SO_4. Evaporation of the solvent gave **26** as a brown solid (322 mg, 0.261 mmol, 70%). ^{1}H NMR (400 MHz, CD_3OD): $\delta=8.81$ (m, 2H), 8.47 (m, 4H), 8.35 (m, 2H), 8.10 (m, 2H), 7.68 (m, 16H), 7.27 (m, 4H), 7.21 (m, 3H), 5.35 (s, 2H), 4.01 (s, 4H), 3.96 (s, 4H), 3.49 (t, $J=$ 6.7 Hz, 4H), 3.30 (m, 8H), 3.18 (t, $J=6.9$ Hz, 2H), 1.92 (m, 6H), 1.33 ppm (s, 9H); ^{13}C NMR (50.3 MHz, CD_3OD): $\delta=167.8$, 166.7, 162.7, 159.6, 159.0, 154.4, 148.8, 148.4, 147.5, 137.2, 135.8, 132.0, 130.2, 128.8, 124.5, 124.2, 123.7, 123.0, 122.9, 122.6, 78.8, 74.1, 73.2, 57.6, 57.2, 37.3, 30.3, 29.12, 7.7 ppm; MS (ESI$^+$): m/z: 621 $[M+2H]^{2+}$, 415 $[M+3H]^{3+}$.

2-(3-Aminopropoxy)-N^1,N^3-bis[3-(6-{[(dipyridin-2-ylmethyl)(pyridin-2-ylmethyl)amino]methyl}nicotinamido)propyl]isophthalamide (28): **26** (320 mg, 0.26 mmol) was dissolved in a mixture of CH_2Cl_2 (10 mL) and TFA (1 mL). After stirring overnight at room temperature, 2 M aqueous NaOH was added until pH > 9. The resulting mixture was stirred for 15 min and then extracted with CH_2Cl_2 (3×20 mL). The combined extracts were washed with water (3×20 mL) and dried over Na_2SO_4. Evaporation of the solvent gave **28** as a yellow solid (200 mg, 0.176 mmol, 68%). ^{1}H NMR (400 MHz, CD_3OD): $\delta=8.81$ (m, 2H), 8.47 (m, 4H), 8.35 (m, 2H), 8.10 (m, 2H), 7.68 (m, 16H), 7.27 (m, 4H), 7.21 (m, 3H), 5.35 (s, 2H), 4.05 (t, $J=6.1$ Hz, 2H), 4.02 (s, 4H), 3.96 (s, 4H), 3.49 (m, 8H), 2.78 (t, $J=6.9$ Hz, 2H), 1.92 ppm (m, 6H); ^{13}C NMR (50.3 MHz, CD_3OD): $\delta=167.9$, 166.8, 162.7, 159.6, 159.1, 154.3, 148.8, 148.4, 147.4, 137.2, 135.7, 131.9, 130.4, 128.8, 124.5, 123.7, 123.0, 122.9, 122.5, 73.3, 57.6, 57.2, 53.6, 37.7, 29.1 ppm; MS (ESI$^+$): m/z: 380 $[M+3H]^{3+}$.

2-[3-(9-Acridinylamino)propoxy]-N^1,N^3-bis(3-{[(6-{[[di(2-pyridinyl)methyl](2-pyridinylmethyl)amino]methyl}-3-pyridinyl)carbonyl]amino}propyl)isophthalamide (6): A mixture of **28** (150 mg, 0.13 mmol), 9-chloroacridine (30 mg, 0.13 mmol), and phenol (1 g, 10 mmol) was heated at 80 °C for 2 h under an N_2 atmosphere. After cooling to room temperature, Et_2O (5 mL) was added and the suspension was stirred for 15 min. The Et_2O was then decanted off and fresh Et_2O (5 mL) was added. The suspension was stirred for a further 5 min. This procedure was repeated

three times. The Et_2O was finally removed and the yellow solid was taken up in CH_2Cl_2 (5 mL). The resulting solution was washed with 2 M aqueous NaOH (3×3 mL) and dried over Na_2SO_4. Evaporation of the solvent gave **6** as a fine yellow solid (170 mg, 0.13 mmol, 99%). A small fraction was purified by preparative RP-HPLC. ^{1}H NMR (400 MHz, CD_3OD): δ = 8.73 (m, 2H), 8.44 (s, 4H), 8.32 (m, 2H), 7.98 (m, 2H), 7.74 (m, 16H), 7.67 (m, 8H), 7.25 (m, 4H), 7.16 (m, 3H), 5.31 (s, 2H), 4.20 (t, J = 5.8 Hz, 2H), 4.08 (t, J = 6.5 Hz, 2H), 3.95 (s, 2H), 3.91 (s, 2H), 3.31 (m, 8H), 2.25 (m, 2H), 1.80 ppm (m, 4H); ^{13}C NMR (50.3 MHz, CD_3OD): δ = 168.0, 166.6, 162.5, 159.5, 159.0, 154.3, 148.8, 148.3, 147.3, 137.2, 135.6, 131.7, 130.6, 128.6, 124.4, 123.6, 122.9, 122.8, 122.5, 74.3, 73.2, 57.6, 57.1, 53.7, 37.1, 31.1, 29.1 ppm; MS (ESI$^+$): m/z: 658 $[M+2H]^{2+}$, 439 $[M+3H]^{3+}$.

N^1,N^3,N^5-Tris(3-{[(6-{[[di(2-pyridinyl)methyl](2-pyridinylmethyl)amino]-methyl}-3-pyridinyl)carbonyl]amino}propyl)benzene-1,3,5-tricarboxamide (7): N4Py-propylamine **9** (93 mg, 0.20 mmol) and **13** (30 mg, 0.067 mmol) were dissolved in CH_2Cl_2 (20 mL) and the mixture was stirred overnight. Saturated aqueous $NaHCO_3$ solution (10 mL) was then added and the layers were separated. The aqueous layer was extracted with CH_2Cl_2 (3× 25 mL) and the combined organic fractions were washed with saturated aqueous $NaHCO_3$ solution (2×10 mL) and dried over Na_2SO_4. Filtration and evaporation of the solvent yielded a light-brown solid, which was further purified on a size-exclusion column (Sephadex LH 20 with MeOH; 200 mL column). It was obtained as a yellow oil (77.87 mg, 0.05 mmol, 75%). ^{1}H NMR (400 MHz, CD_3OD): δ = 8.81 (d, J = 1.8 Hz, 3H), 8.45 (d, J = 4.6 Hz, 6H), 8.35 (d, J = 4.7 Hz, 3H), 8.32 (m, 3H), 8.09 (m, 3H), 7.96 (m, 3H), 7.80–7.63 (m, 15H), 7.52 (m, 3H), 7.26 (m, 6H), 7.19 (m, 3H), 5.26 (s, 3H), 4.01 (s, 6H), 3.96 (s, 6H), 3.40 (m, 12H), 1.97–1.83 ppm (m, 6H); ^{13}C NMR (50 MHz, CD_3OD): δ = 168.67, 167.88, 163.83, 160.77, 160.24, 149.98, 149.52, 148.61, 138.36, 136.88, 136.67, 129.93, 125.63, 124.80, 124.18, 124.02, 123.63, 74.40, 58.75, 58.36, 38.52, 38.34, 30.17 ppm; MS (ESI$^+$): m/z: 1558.3 $[M+H]^+$, 780.1 $[M+2H]^{2+}$, 520.5 $[M+3H]^{3+}$.

4-{2-(3-{[(6-{[[Di(2-pyridinyl)methyl](2-pyridinylmethyl)amino]methyl}-3-pyridinyl)carbonyl]amino}propyl)-2-oxoethyl}-N^1,N^7-bis(3-{[(6-{[[di(2-pyridinyl)methyl](2-pyridinylmethyl)amino]methyl}-3-pyridinyl)carbonyl]-amino}propyl)heptanediamide (8): A solution of propylamine-N4Py derivative **9** (0.10 g, 0.214 mmol), 4-(carboxymethyl)heptanedioic acid **17** (15.08 mg, 0.069 mmol), and HOBt (28.94 mg, 0.214 mmol) in CH_2Cl_2 (7.5 mL) was cooled to 0 °C. EDC (59.84 mg, 0.312 mmol) and *N*,*N*-diisopropylethylamine (27.8 mg, 0.215 mmol) were then added and the reaction mixture was stirred for 1 h at 0 °C and at room temperature overnight. The mixture was then washed with saturated aqueous $NaHCO_3$ solution (2×10 mL) and water (10 mL). The organic phase was dried over Na_2SO_4, filtered, and concentrated to afford a light-yellow solid, which was further purified on a size-exclusion column (Sephadex LH 20 with MeOH; 200 mL column) to yield **8** (97.1 mg, 0.062 mmol, 90%). ^{1}H NMR (300 MHz, CD_3OD): δ = 8.88 (dd, J = 4.6, 1.5 Hz, 3H), 8.48 (d, J = 4.1 Hz, 6H), 8.38 (d, J = 3.2 Hz, 3H), 8.27–8.15 (m, 6H), 8.07 (t, J = 7.7 Hz, 6H), 7.70–7.35 (m, 27H), 7.17–6.95 (m, 6H), 5.33 (s, 3H), 3.97 (s, 6H), 3.92 (s, 6H), 3.48–3.31 (m, 12H), 1.74–1.47 ppm (m, 6H); ^{13}C NMR (126 MHz, CD_3OD): δ = 176.2, 175.3, 167.8, 163.8, 160.8, 160.2, 150.0, 149.5, 148.6, 138.6, 138.5, 137.0, 130.0, 128.3, 126.6, 125.7, 124.9, 124.3, 124.1, 123.8, 74.6, 58.8, 58.5, 41.6, 38.4, 37.9, 36.1, 34.3, 30.7, 30.2 ppm; MS (ESI$^+$): m/z: 523.2 $[M+3H]^{3+}$, 392.7 $[M+4H]^{4+}$.

Titration studies of $(NH_4)_2Fe^{II}(SO_4)_2$ and 3: For ^{1}H NMR titrations, 0, 1, 2, or 3 equivalents of $(NH_4)_2Fe^{II}(SO_4)_2$ were added to a solution of **3** in D_2O (with acetone as internal standard) (Figure 2a). The ^{1}H NMR spectra were referenced with respect to the acetone peak (δ = 2.22 ppm), since the residual solvent peak of D_2O tends to shift after the addition of the $(NH_4)_2Fe^{II}(SO_4)_2$. The relative area of the two absorptions between δ = 25 and 28 ppm compared to that of the acetone peak was plotted against the number of equivalents of $(NH_4)_2Fe^{II}(SO_4)_2$ (Figure 2b).

For UV/Vis titration, 0, 1, 2, or 3 equivalents of $(NH_4)_2Fe^{II}(SO_4)_2$ were added to a solution of **3** in H_2O (Figure 3a. The relative extinction coefficient ($\varepsilon/\varepsilon_{max}$) was plotted against the number of equivalents of $(NH_4)_2Fe^{II}(SO_4)_2$ (Figure 3b).

Acknowledgement

We thank Dr. R. M. Scheek for useful discussions, and the Netherlands Research School on Catalysis (NRSC-Catalysis) for financial support.

[1] H. Umezawa, K. Maeda, T. Takeuchi, Y. Okami, *J. Antibiot.* **1966**, *19*, 200.
[2] R. M. Burger, *Chem. Rev.* **1998**, *98*, 1153.
[3] S. M. Hecht, *Bleomycin: Chemical, Biochemical and Biological Aspects*, Springer, New York, **1979**.
[4] S. M. Hecht, *J. Nat. Prod.* **2000**, *63*, 158.
[5] W. K. Pogozelski, T. D. Tullius, *Chem. Rev.* **1998**, *98*, 1089.
[6] L. F. Povirk, W. Wübker, W. Köhnlein, F. Hutchinson, *Nucleic Acids Res.* **1977**, *4*, 3573.
[7] J. Y. Chen, J. Stubbe, *Nat. Rev. Cancer* **2005**, *5*, 102.
[8] D. Freifelder, B. Trumbo, *Biopolymers* **1969**, *7*, 681.
[9] A. Decker, M. S. Chow, J. N. Kemsley, N. Lehnert, E. I. Solomon, *J. Am. Chem. Soc.* **2006**, *128*, 4719.
[10] L. Thompson, C. Limoli, C. Origin, *Recognition, signaling and repair of DNA double strand mammalian cells*, Springer, New York, **2003**.
[11] R. J. Guajardo, S. E. Hudson, S. J. Brown, P. K. Mascharak, *J. Am. Chem. Soc.* **1993**, *115*, 7971.
[12] C. Hemmert, M. Pitié, M. Renz, H. Gornitzka, S. Soulet, B. Meunier, *J. Biol. Inorg. Chem.* **2001**, *6*, 14.
[13] R. P. Hertzberg, P. B. Dervan, *J. Am. Chem. Soc.* **1982**, *104*, 313.
[14] P. Mialane, A. Nivorojkine, G. Pratviel, L. Azéma, M. Slany, F. Godde, A. Simaan, F. Banse, T. Kargar-Grisel, G. Bouchoux, J. Sainton, O. Horner, J. Guilhem, L. Tchertanova, B. Meunier, J. J. Girerd, *Inorg. Chem.* **1999**, *38*, 1085.
[15] M. Pitié, C. Boldron, G. Pratviel, *Adv. Inorg. Chem.* **2006**, *58*, 77.
[16] E. L. M. Wong, G. S. Fang, C. M. Che, N. Y. Zhu, *Chem. Commun.* **2005**, 4578.
[17] J. J. Hayes, *Biochemistry* **1996**, *35*, 11931.
[18] C. Marchand, C. H. Nguyen, B. Ward, J. S. Sun, E. Bisagni, T. Garestier, C. Hélène, *Chem. Eur. J.* **2000**, *6*, 1559.
[19] M. Roy, B. Pathak, A. K. Patra, E. D. Jemmis, M. Nethaji, A. R. Chakravarty, *Inorg. Chem.* **2007**, *46*, 11122.
[20] G. C. Silver, W. C. Trogler, *J. Am. Chem. Soc.* **1995**, *117*, 3983.
[21] Q. Jiang, N. Xiao, P. F. Shi, Y. G. Zhu, Z. J. Guo, *Coord. Chem. Rev.* **2007**, *251*, 1951–1972.
[22] R. P. Hertzberg, P. B. Dervan, *Biochemistry* **1984**, *23*, 3934–3945.
[23] Oxidative double-strand cleavage has been reported with Cu complexes, albeit with high copper/DNA base pair ratios: a) F. V. Pamatong, C. A. Detmer, J. R. Bocarsly, *J. Am. Chem. Soc.* **1996**, *118*, 5339; b) Y. Jin, J. A. Cowan, *J. Am. Chem. Soc.* **2005**, *127*, 8408; c) J. He, P. Hu, Y. J. Wang, M. L. Tong, H. Z. Sun, Z. W. Mao, L. N. Ji, *Dalton Trans.* **2008**, 3207.
[24] G. Roelfes, M. E. Branum, L. Wang, L. Que, B. L. Feringa, *J. Am. Chem. Soc.* **2000**, *122*, 11517.
[25] M. Lubben, A. Meetsma, E. C. Wilkinson, B. Feringa, L. Que, *Angew. Chem.* **1995**, *107*, 1610; *Angew. Chem. Int. Ed. Engl.* **1995**, *34*, 1512.
[26] G. Roelfes, V. Vrajmasu, K. Chen, R. Y. N. Ho, J. U. Rohde, C. Zondervan, R. M. la Crois, E. P. Schudde, M. Lutz, A. L. Spek, R. Hage, B. L. Feringa, E. Munck, L. Que, *Inorg. Chem.* **2003**, *42*, 2639.
[27] For hydrolytic double-strand cleavage with a dinuclear iron complex, see: R. X. Q. Chen, X. J. Peng, J. Y. Wang, Y. Wang, S. Wu, L. Z. Zhang, T. Wu, Y. K. Wu, *Eur. J. Inorg. Chem.* **2007**, 5400.
[28] T. A. van den Berg, B. L. Feringa, G. Roelfes, *Chem. Commun.* **2007**, 180.
[29] K. J. Humphreys, K. D. Karlin, S. E. Rokita, *J. Am. Chem. Soc.* **2001**, *123*, 5588.
[30] K. J. Humphreys, A. E. Johnson, K. D. Karlin, S. E. Rokita, *J. Biol. Inorg. Chem.* **2002**, *7*, 835.
[31] K. J. Humphreys, K. D. Karlin, S. E. Rokita, *J. Am. Chem. Soc.* **2002**, *124*, 8055.
[32] K. J. Humphreys, K. D. Karlin, S. E. Rokita, *J. Am. Chem. Soc.* **2002**, *124*, 6009.

[33] T. Ito, S. Thyagarajan, K. D. Karlin, S. E. Rokita, *Chem. Commun.* **2005**, 4812.
[34] L. Li, K. D. Karlin, S. E. Rokita, *J. Am. Chem. Soc.* **2005**, *127*, 520.
[35] L. Li, N. N. Murthy, J. Telser, L. N. Zakharov, G. P. A. Yap, A. L. Rheingold, K. D. Karlin, S. E. Rokita, *Inorg. Chem.* **2006**, *45*, 7144.
[36] S. Thyagarajan, N. N. Murthy, A. A. N. Sarjeant, K. D. Karlin, S. E. Rokita, *J. Am. Chem. Soc.* **2006**, *128*, 7003.
[37] Y. M. Zhao, J. H. Zhu, W. J. He, Z. Yang, Y. G. Zhu, Y. Z. Li, J. F. Zhang, Z. J. Guo, *Chem. Eur. J.* **2006**, *12*, 6621.
[38] L. C. Chan, B. G. Cox, *J. Org. Chem.* **2007**, *72*, 8863.
[39] See also the Supporting Information.
[40] The first term of a Poisson distribution predicts that the amount of linear DNA will reach a maximum at around 37%; in practice, this means that significant amounts of a smear are produced in the gel, which precludes quantitative analysis.
[41] See the Experimental Section: Equations (1) and (2).
[42] G. Roelfes, Ph.D. Thesis, Rijksuniversiteit Groningen, **2000**.

Received: July 11, 2008
Revised: September 29, 2008
Published online: January 7, 2009

